IOP Publishing Modelling and Simulation in Materials Science and Engineering

Modelling Simul. Mater. Sci. Eng. **24** (2016) 075005 (15pp) doi:10.1088/0965-0393/24/7/075005

A Markov random field approach for modeling spatio-temporal evolution of microstructures

Pinar Acar and Veera Sundararaghavan

Aerospace Engineering, University of Michigan, Ann Arbor, MI, USA

E-mail: veeras@umich.edu

Received 10 March 2016, revised 16 June 2016
Accepted for publication 18 July 2016
Published 9 September 2016

Abstract

The following problem is addressed: 'Can one synthesize microstructure evolution over a large area given experimental movies measured over smaller regions?' Our input is a movie of microstructure evolution over a small sample window. A Markov random field (MRF) algorithm is developed that uses this data to estimate the evolution of microstructure over a larger region. Unlike the standard microstructure reconstruction problem based on stationary images, the present algorithm is also able to reconstruct time-evolving phenomena such as grain growth. Such an algorithm would decrease the cost of full-scale microstructure measurements by coupling mathematical estimation with targeted small-scale spatiotemporal measurements. The grain size, shape and orientation distribution statistics of synthesized polycrystalline microstructures at different times are compared with the original movie to verify the method.

Keywords: microstructure, reconstruction, probability, markov random fields

(Some figures may appear in colour only in the online journal)

1. Introduction

Images of polycrystalline microstructures are routinely obtained using diffraction or optical methods over small spatial domains. Using reconstruction methods, microstructural maps over larger spatial regions can be generated. Most popular among these methods are feature-based algorithms that attempt to match features (such as marginal histograms [1], multiresolution filter outputs (Gaussian [2] and wavelet [3] filters) and point probability functions (eg. autocorrelation function) [4–7]) with the experimental image. These methods are good at capturing global features of the image, however local information in the form of per-pixel

data is lost. Thus, features such as grain boundaries are smeared out when reconstructing polycrystalline structures [3].

In an earlier paper [8], we demonstrated the use of Markov random field (MRF) algorithms to alleviate this issue. The algorithm works by sampling the conditional probability density for the coloring of a pixel given the known states of its neighboring pixels using reference experimental images. If only the nearest neighbors are chosen, this amounts to sampling from a Ising-type model [10]. While in Ising models, a lattice is constructed with pixels (with binary states) interacting with its nearest neighbors, in MRFs, pixels take up integer or vector states and interact with multiple neighbors over a window. The sampling of conditional probability of a pixel given the states of its known neighbors is based on Claude Shannon's generalized Markov chain [11]. In the one dimensional problem, a set of consecutive pixels is used as a template to determine the probability distribution function (PDF) of the next pixel. In 2D microstructures, microstructures are grown layer-by-layer from a small seed image (3×3 pixels) taken randomly from the experimental micrograph [12]. The algorithm first finds all windows in an experimental micrograph that are similar to an unknown pixel's neighborhood window. One of these matching windows is chosen and its center pixel is taken to be the newly synthesized pixel. This technique is popular in the field of 'texture synthesis' [12–15], in geological material reconstruction literature where such sampling methods are termed 'multiple-point statistics' [16], and more recently, has been applied for modeling 2D material microstructures [8, 9]. However, these methods were primarily developed for stationary microstructure images.

Advanced high-speed imaging techniques are now able to routinely obtain movies of microstructure evolution over small spatial domains. It will be valuable to develop similar reconstruction methods to recover the *temporal evolution* of microstructures over a larger spatial domain (or perhaps, the entire specimen) from this data. In this paper, we extend the sampling algorithm in [8] to also allow for temporal reconstruction of various frames in a movie. This is done by employing an optimization technique that ensures contiguous evolution of grain boundaries across consecutive frames. The optimization approach minimizes a neighborhood cost function that ensures that the local neighborhood of the current frame is similar to some neighborhood of the corresponding experimental frame. Such an optimization strategy has been previously used in the context of 3D microstructure reconstruction in [17, 18] but not for temporal microstructure reconstruction, to the best of our knowledge.

The limited nature of experimental data is due to small regions (order of microns) that are usually measured while engineering analysis is over much large domains (order of centimeters) (see figure 1). The method presented in this paper is capable of reconstructing larger regions of microstructure needed for engineering analysis by using small-scale experimental data. We assume that the 'limited' experimental data contains a sufficient range of features to capture the true larger scale microstructure. The major contribution of this paper, compared to large literature of statistical reconstruction methods [4], is (1) the capability of predicting not only the spatial evolution but also the temporal evolution of 2D microstructures (2) Ability to work with polycrystalline microstructure while most literature is for multi-phase random composites. We employ the method for generating grain growth movies using results from a small phase field simulation. The results are tested by comparing statistical measures across various time steps with the original movie.

2. Mathematical modeling of microstructures as Markov random fields

Some of early attempts at microstructure modeling were based on Ising models [10]. In the Ising model, a $N \times N$ lattice (L) is constructed with values X_i assigned for each particle i on the lattice, $i \in [1, .., N^2]$. In an Ising model, X_i is a binary variable equal to either $+1$ or -1

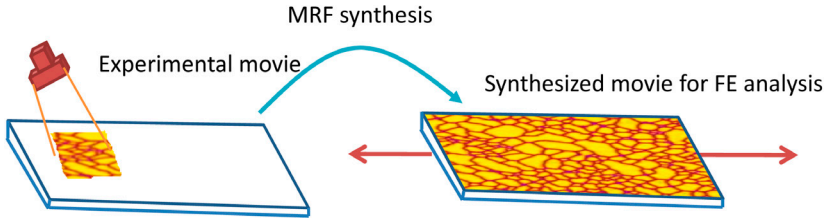

Figure 1. The objective of the MRF algorithm is to reconstruct larger domains from small measurement volumes. The reconstructed microstructure can be used for engineering finite element (FE) analysis.

(eg. magnetic moment [10]). In general, the values X_i may contain any one of G color levels in the range $\{0,1,..,G-1\}$ (following the integer range extension of the Ising model by Besag [19]). A *coloring* of L denoted by $\boldsymbol{X}$ maps each particle in the lattice L to a particular value in the set $\{0,1,..,G-1\}$. Ising models fall under the umbrella of *undirected graph models* in probability theory. In order to rewrite the Ising model as a graph, we assign neighbors to particles and link pairs of neighbors using a bond as shown in figure 2(a). The rule to assign neighbors is based on a *pairwise Markov property*. A particle j is said to be a neighbor of particle i only if the conditional probability of the value X_i given all other particles (except (i,j), i.e. $p(X_i|X_1, X_2, .., X_{i-1}, X_{i+1}, .., X_{j-1}, X_{j+1}, .., X_{N^2})$) depends on the value X_j.

In the classical Ising model, each particle is bonded to the next nearest neighbor as shown in figure 2(a). For modelling microstructures, a higher order Ising model (figure 2(b)) is used. The particles of the lattice correspond to pixels of the 2D microstructure image. The neighborhood of a pixel is modeled using a square window around that pixel and bonding the center pixel to every other pixel within the window. Using this graph structure, a *Markov random field* can be defined as the joint probability density $P(\boldsymbol{X})$ on the set of all possible colorings $\boldsymbol{X}$, subject to a *local Markov property*. The *local Markov property* states that the probability of value X_i, given its neighbors, is conditionally independent of the values at all other particles. In other words, $P(X_i|\text{all particles except } i) = p(X_i|\text{neighbors of particle } i)$. Next, we describe a method based on [8] to sample from the conditional probability density $p(X_i|\text{neighbors of voxel } i)$.

2.1. Sampling algorithm

In the following discussion, the color (X_i) of a pixel i is represented using G color levels in the range $\{0,1,..,G-1\}$ each of which maps to an RGB triplet. The number of color levels is chosen based on the microstructure to be reconstructed, eg. for binary images $G = 2$. Let $\boldsymbol{E}$ and $\boldsymbol{S}$ denote the experimental and synthesized microstructure, respectively. Let v be a pixel in $\boldsymbol{S}$ whose color needs to inferred using the sampling procedure. Let $\boldsymbol{S}_v$ denote the colors in a neighborhood window around pixel v. Let $\boldsymbol{E}^w$ denote the colors of pixels in a window of the same size in the input 2D micrograph.

In order to find the coloring of pixel v, one needs to compute the conditional probability density $p(X_v|\boldsymbol{S}_v)$. Explicit construction of such a probability density is often computationally intractable. Instead, the most likely value of v is identified by first finding a window $\boldsymbol{E}_v$ in the input 2D micrograph that is most similar to $\boldsymbol{S}_v$ (see figure 3). This is done by solving the following problem (where $\boldsymbol{S}_{v,u}$ denotes the color of pixel u in $\boldsymbol{S}_v$ and $\boldsymbol{E}_u^w$ denotes the color of pixel u in $\boldsymbol{E}^w$):

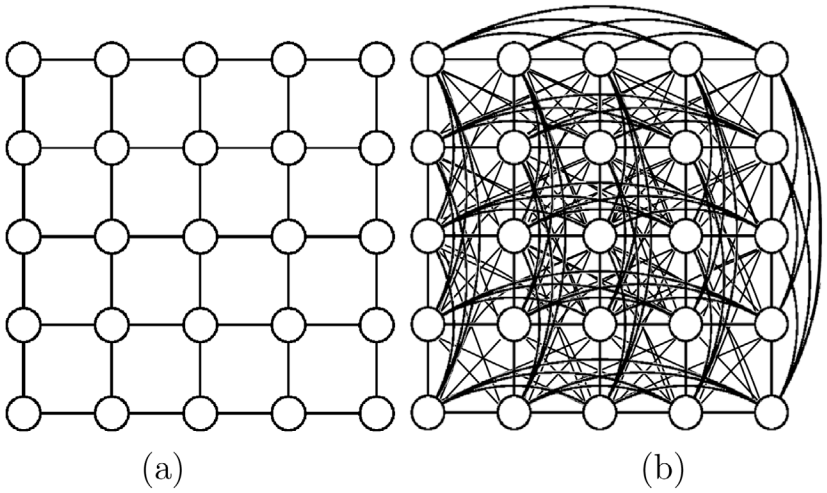

Figure 2. Markov random field as an undirected graph model, circles are pixels in the image and bonds are used to connect neighbors: (a) Ising model with nearest neighbor interactions. (b) Microstructure modeled by including higher order interactions in the Ising model.

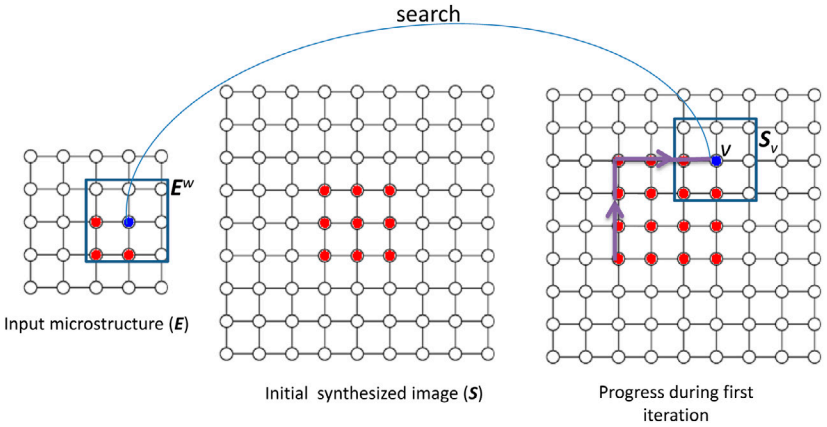

Figure 3. The Markov random field approach: the image is grown from a 3×3 seed image (center). As the algorithm progresses along the path shown (right), the unknown output pixel (shown in blue) is computed by searching for a pixel with a similar neighborhood in the input image (left).

$$\boldsymbol{E}_v = \arg\min_{\boldsymbol{E}^w} \sum_u \omega_{v,u}(\boldsymbol{S}_{v,u} - \boldsymbol{E}_u^w)^2 \tag{1}$$

where, $D = \sum_u \omega_{v,u}(\boldsymbol{S}_{v,u} - \boldsymbol{E}_u^w)^2$ is a distance measure defined as the normalized sum of weighted squared differences of pixel colors. In order to preserve the short range correlations of the microstructure as much as possible, the weight for nearby pixel is taken to be greater than pixels farther away (Gaussian weighting function ω is used). If the pixel u is located at position (x,y) (in lattice units) with respect to the center pixel v (located at (0,0)), $\omega_{v,u}$ is given as:

$$\omega_{v,u} = \frac{\exp(-\frac{(x^2+y^2)}{2\sigma^2})}{\sum_i \sum_j \exp(-\frac{(i^2+j^2)}{2\sigma^2})} \tag{2}$$

Here, the summation in the denominator is taken over all the known pixels in $\boldsymbol{S}_v$. The weights $\omega_{v,u}$ for the unknown pixels in $\boldsymbol{S}_v$ are taken to be zero. This ensures that the distance measure is computed only using the known values and is normalized by the total number of known pixels. The standard deviation (σ) is taken to be $0.16w$.

The problem in equation (1) is solved using an exhaustive search by comparing all the windows in the input 2D micrograph to the corresponding neighborhood of pixel v. In our approach, a measure of stochasticity is introduced by storing all matches with a distance measure that is within 1.3 times that of the best matching window [12]. The center pixel colors of all these matches give a histogram for the color of the unknown pixel (X_v), which is then sampled using a uniform random number.

The microstructure is grown layer-by-layer starting from a small seed image (3×3 pixels) taken randomly from the experimental micrograph (figure 3). In this way, for any pixel the values of only some of its neighborhood pixels will be known. The fundamental approximation in this numerical implementation is that the probability distribution function (PDF) of an unfilled pixel is assumed to be independent of the PDF of its unfilled neighbors. Each iteration in the algorithm involves coloring the unfilled pixels along the boundary of filled pixels in the synthesized image as shown in figure 3. An upper limit of 0.1 is enforced for the distance measure initially. If the matching window for a unfilled pixel has a larger distance measure, then the pixel is temporarily skipped while the other pixels on the boundary are filled. If none of the pixels on the boundary can be filled during an iteration, then the threshold is increased by 10% for the next iteration.

2.2. Temporal sampling

Consider an input microstructure movie which is a collection of F frames. In the temporal reconstruction algorithm, the first frame is reconstructed using the algorithm in section 2.1. The reference locations (in the experimental frame) of each pixel in the synthesized microstructure is stored. The Nth synthesized frame is computed by updating the $(N-1)$th synthesized frame using pixels at the previously stored locations in the Nth experimental frame. As the microstructure evolves, the reference locations may change. To update the stored reference locations, an optimizer is used on the Nth synthesized frame. The optimization is posed as a minimization of an energy function [20, 21]:

$$\boldsymbol{S}^* = \arg\min_{\boldsymbol{S}} \sum_v \sum_u \omega_{v,u}(\boldsymbol{S}_{v,u} - \boldsymbol{E}_{v,u})^2 \tag{3}$$

where, $\boldsymbol{S}^*$ is the optimum synthetic microstructure. The optimization is carried out in two steps. In the first step, the energy is minimized with respect to $\boldsymbol{E}_v$. This step is identical to the sampling algorithm (equation (1)) and finds the best matching neighborhood of each pixel v by solving the following problem:

$$\boldsymbol{E}_v = \arg\min_{\boldsymbol{E}^w} \sum_u \omega_{v,u}(\boldsymbol{S}_{v,u} - \boldsymbol{E}^w_u)^2 \tag{4}$$

This is an exhaustive search (as previously explained in the sampling algorithm) that finds a matching experimental image neighborhood for each pixel v in the synthesized image. Because the matching neighborhoods contain other pixels too, multiple values of coloring are obtained

for each pixel depending on how many windows overlap over that pixel. The optimal color of pixel v is computed by setting the derivative of the energy function equation (3) with respect to X_v to zero. This leads to a simple weighted average expression for the color of pixel v:

$$X_v = (\sum_u \omega_{u,v} \boldsymbol{E}_{u,v})/(\sum_u \omega_{u,v}) \tag{5}$$

Note that the subscripts u and v are switched in the above expression as compared to equation (3). This implies that the optimal color of the pixel v is the weighted average of the colors at locations corresponding to pixel v in the best matching windows ($\boldsymbol{E}_u$) of pixels (u) in the synthesized microstructure. Since X_v changes after this step, the set of closest input neighborhoods $\boldsymbol{E}_v$ will also change. Hence, these two steps were repeated until convergence, i.e. until the set $\boldsymbol{E}_v$ stops changing. To get optimal reconstruction speed, the optimizer is only used once every k frames, where k is specified by the user. The pseudocode in table 1 summarizes the solution procedure and temporal sampling scheme.

3. Examples

3.1. Synthesis of a gray scale movie

The temporal Markov random field (MRF) algorithm is used to synthesize the evolution of microstructure over a larger region given a small input movie. The movie is obtained from a phase field simulation of grain growth [22]. The image size of the original gray-scale movie is 71×71. The synthesized movies are double the size (142×142 pixels) but over the same time steps as the original phase field simulation. The snapshots from the original phase field simulation and the synthesized movies for initial, an intermediate and the final time are compared in figure 4. These synthesized microstructures correspond to window sizes of 5, 7 and 9 used in the MRF model. The window size is the adjustable parameter in the method for different microstructures. At window sizes much smaller than the correlation lengths, false matches lead to high noise in the reconstructions. The window size of 5 does not produce a good quality reconstruction as seen in the clusters of small grains that persist at longer times. At very high window sizes, not enough matching windows can be identified and in addition, more computations are needed that slow down the simulation. Hence, there is an ideal window size that needs to be found either through numerical trial or using correlation lengths as shown in [9, 23] for two phase materials. As seen in figure 4, the window sizes of 7 and 9 visually look similar to the phase field simulation. To quantitatively compare the grain size and shapes of the input and synthesized images, two global feature vectors were extracted from the input microstructure and compared to the synthesized microstructure (window size 9). The feature vectors are described below:

(i) Grain size and grain boundary perimeter statistics [24, 25]: the grain size and grain boundary (GB) perimeter of each grain is tabulated. A histogram containing the area or the perimeter of grains in the x-axis and the fraction of grains with the corresponding area (or GB perimeter) is plotted in the y-axis.

(ii) Grain shape statistics using the Rose of intersections [26]: to obtain the rose of intersections, a network of parallel equidistant lines is placed over the microstructure image at several angles and the number of grain boundary intersections with each test line is measured. The histogram of intersections with the angle of orientation of the lines is called the rose of intersection. Rose of interactions is related to the ASTM standard for determining the average grain size (E,112-188, also see Heyn intercept technique [27]).

Table 1. Pseudocode for the MRF microstructure evolution algorithm.

Given a movie consisting of *N* frames
Step 1. Reconstruct frame 1 by sampling
– Initialize synthesized frame any 3×3 patch from the 1st input frame
– Initialize the location matrix using input frame coordinates of the patch.
– Initialize threshold $= 0.1$
– Set window size $= w \times w$ pixels
While [the synthesized image is not complete] **do**
For all unfilled neighbors

Get the image window around the unfilled pixel
Find the window with lowest D (see equation (1) with weights in equation (2), $\sigma = 0.16w$)
Find all matching windows within 1.3 times D
Pick one match using a uniform random number

If distance of the match $<$ threshold
The unfilled pixel is filled using the center pixel of the matching window
Store coordinates of center pixel in the location matrix
Otherwise
Skip and continue to next unfilled neighbor
end if

If none of the neighbors are filled
Raise threshold by 10%
end if

end for
end while
Step 2. Reconstruct all other frames
For frames $i = 2,..,N$
– Generate ith frame using pixels at stored locations in the ith input frame
For every k frames ($k = 5$ here)
Find the best matching windows in ith input frame (equation (4))
Store locations of the center pixels of these matching windows
Use equation (5) to recompute the value of pixels in the ith synthesized frame.
end for
end for

The shape and size of the rose of intersections is related to the average shape and size of the grains in the microstructure.

The plot in figures 5(a) and (b) shows the fraction of grains as a function of grain area and grain perimeter (measured in pixels) for initial and final times. The rose of intersections graphs are illustrated using lines with 11 different angles at initial and final times. The shape histogram depicts the decrease in overall grain size with time (shrinking of the contour) while the overall grain shape as indicated by the contour shape remains mostly equiaxial. Figure 5 shows that the synthesized microstructures are able to capture the grain size and shape statistics of the original microstructure evolution predicted by the phase field method. MRF

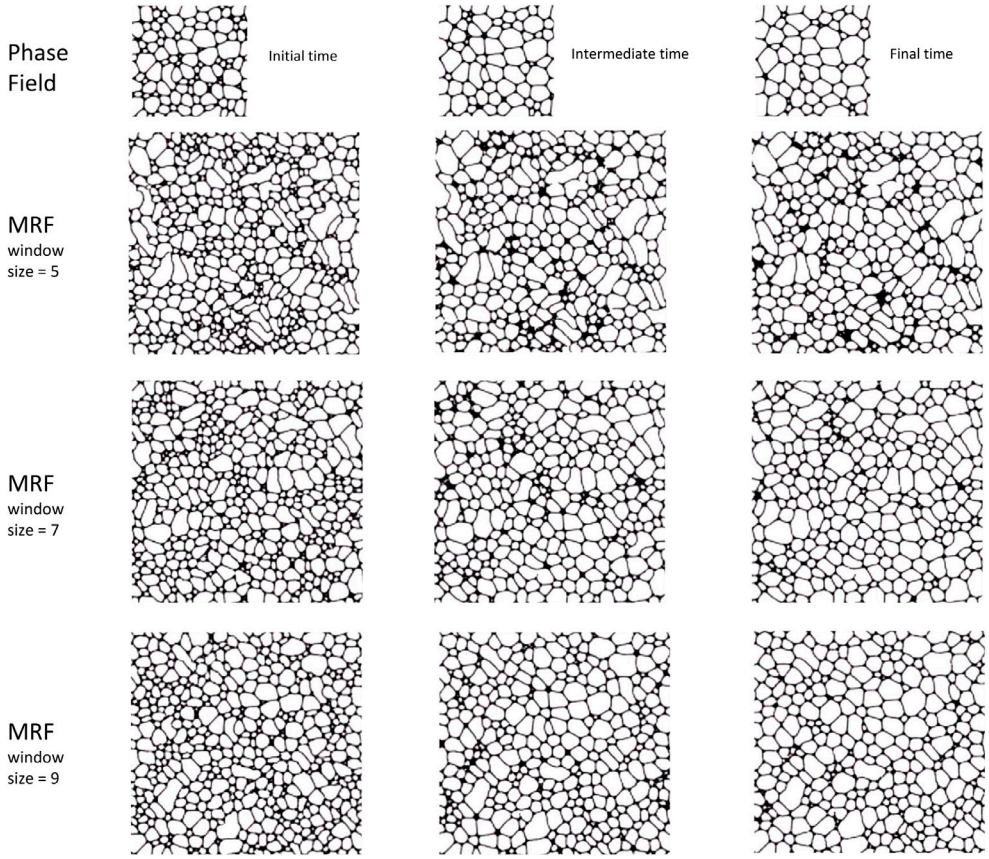

Figure 4. Snapshots of the gray-scale movie are compared to the synthesized movie snapshots at initial, intermediate and final times. The synthesized microstructures are obtained using three different window sizes.

sampling approach proposed here is significantly faster than performing a phase field simulation for larger spatial regions. We do not solve any differential equations and as such, are not constrained by the small time increments needed to maintain numerical stability.

3.2. Synthesis of a colored microstructure movie

The second example includes crystal orientation information (in the form of grain coloring) in addition to grain sizes and shapes. The original movie (downloadable from [28]) illustrates grain growth in a 2D microstructure generated from a cellular automata method. The synthesized movies are generated using window sizes of 5, 7 and 9 respectively, and the number of time frames is the same as the original movie. The image size of the original movie is 87×106 pixels, and the synthesized images are twice the size of the original. The time snapshots were taken for initial, intermediate and final times, and are shown in figure 6. A visual check of the movie indicates that the synthesized microstructures capture the grain growth behavior in a larger spatial domain and the snapshots at different times look qualitatively similar with respect to grain sizes and shapes of the original cellular automata simulation (figure 6) for window sizes of 7 and 9.

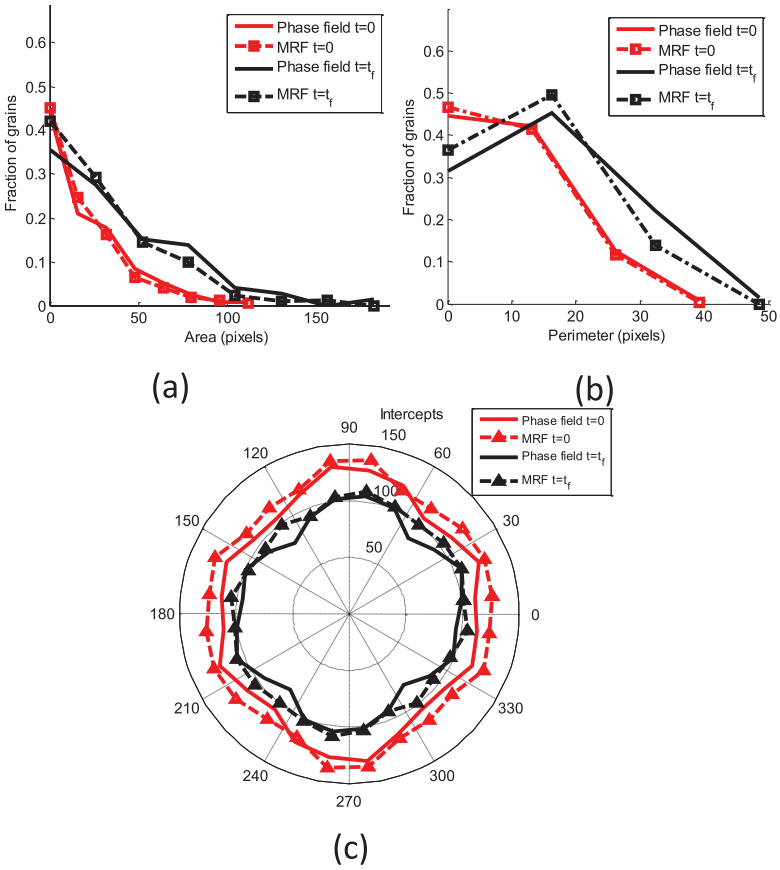

Figure 5. Comparison of statistical features of phase field and MRF algorithms ((a) and (b)) grain area and grain perimeter statistics at initial and final time (c) Rose of interactions at initial and final time.

To measure the similarity of coloring of the sample and synthesized microstructures, we assigned a unique orientation to each pixel based on its color and have plotted the orientation distribution function in figure 7. The orientation distribution function (ODF), in principle, is equivalent to a color histogram and contains the volume density of each crystal orientation (color) in the Rodrigues fundamental region for a copper polycrystal [29]. The ODFs are plotted for the sample and three synthesized images (window sizes of 5, 7, 9 in the MRF model) at the initial and final times. Once the crystal orientation distribution is known, properties such as Young's modulus can be computed and compared. In particular, we are interested in the anisotropy of Young's modulus with respect to loading direction predicted by the original and synthesized image.

Values of elastic parameters for FCC copper crystal are taken as $c_{11} = 168.0\,\text{GPa}$, $c_{12} = 121.4\,\text{GPa}$, $c_{44} = 75.4\,\text{GPa}$ [30]. The polycrystal stiffness, $\bar{\boldsymbol{C}}$, is computed through a weighted average of the stiffness of individual crystals expressed in the sample reference frame over the fundamental region. The elastic modulus is then computed through this polycrystal stiffness as $\boldsymbol{E} = \frac{1.0}{(\bar{\boldsymbol{C}}^{-1})_{(11)}}$. Furthermore, the elastic modulus during loading at any angle

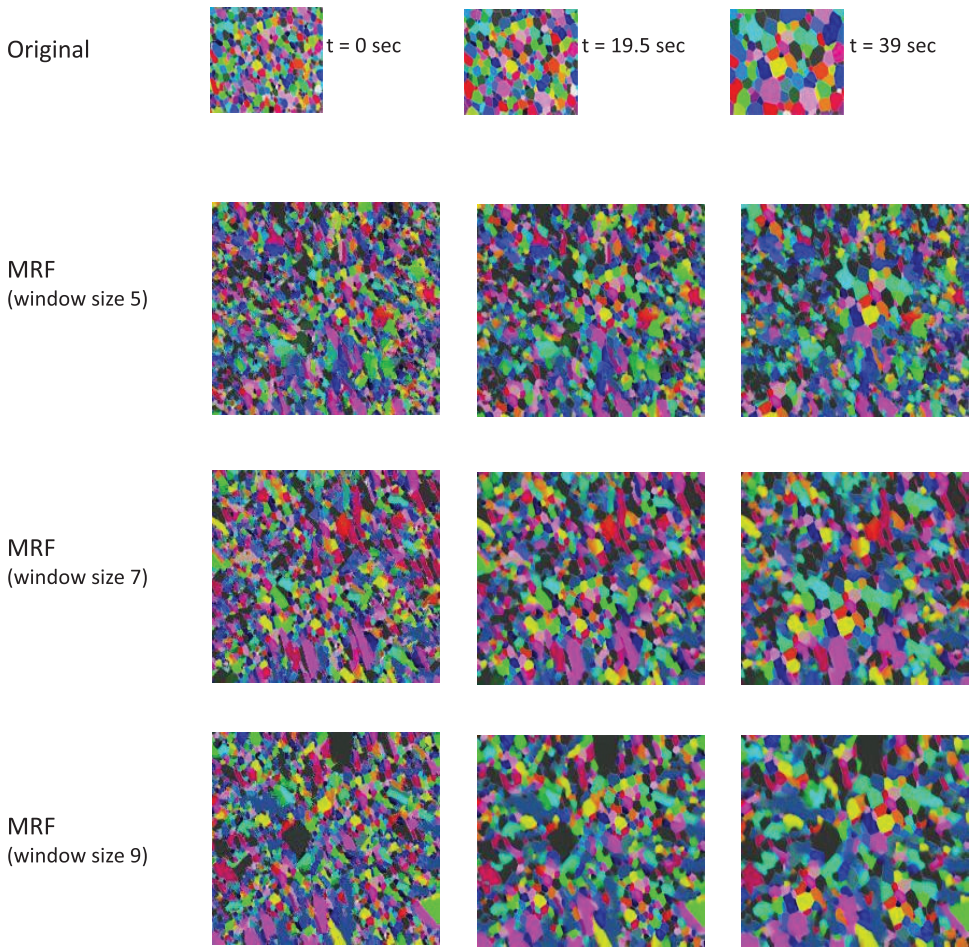

Figure 6. Time snapshots of the colored movie.

with respect to the rolling direction (RD) can be evaluated using the above equation, but after a coordinate transformation of $\bar{\boldsymbol{C}}$. The distributions of Young's modulus with respect to the different loading angles is given in figure 8 for initial and final time snapshots. The trend in elastic modulus anisotropy is similar for both original and synthesized images, with minimum modulus for loading at 45 degrees to the rolling direction. The differences in the values of Young's modulus at specific loading angles may be attributed to the stochasticity introduced by the reconstruction algorithm. In addition, the Young's modulus predicted by reconstruction using window sizes 5, 7 and 9 show a converging trend, and such a trend may be used for optimal window size selection.

3.3. Synthesis of microstructure evolution with non-uniform grain growth

The last example includes a microstructure movie showing heterogeneous distribution of grain sizes and shapes. The original movie (downloadable from [31]) is generated from a phase field simulation, and it illustrates the presence of two different grain sizes at any time step with a few grains evolving in an anisotropic fashion. This example is used to illustrate window size

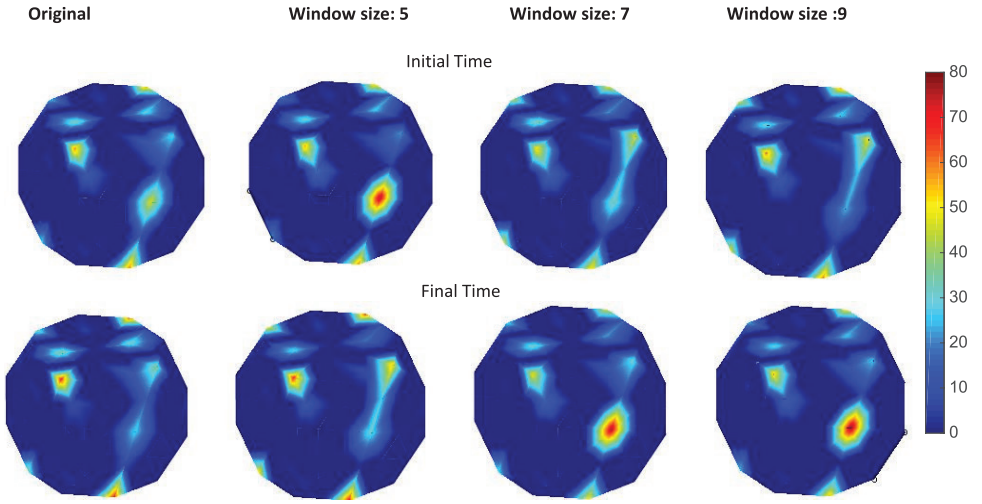

Figure 7. ODF representations at initial and final times.

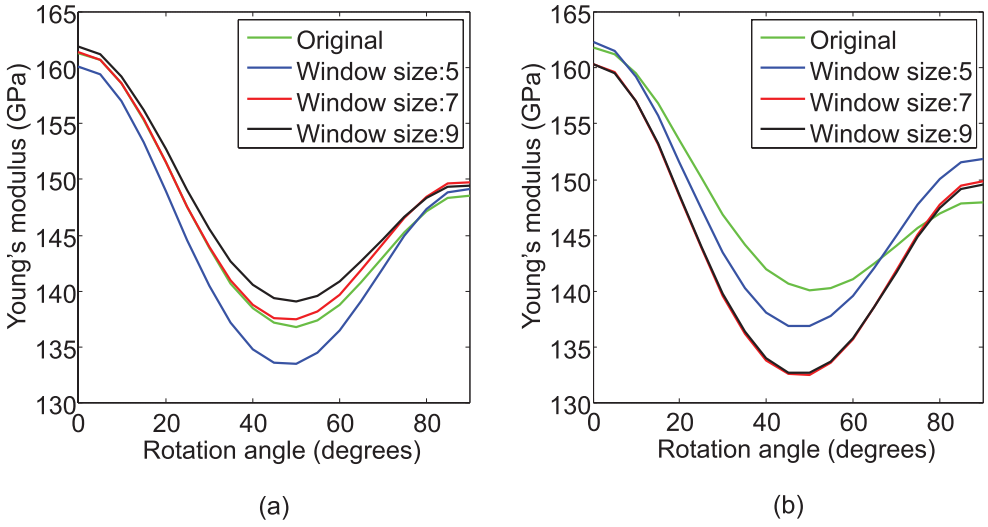

Figure 8. Young's modulus distributions: (a) for initial time snapshot, (b) for final time snapshot.

selection based on correlation functions. The original movie is sized to 75×75 pixel grid and the synthesized movies are generated for a 150×150 domain using window sizes of 5, 7 and 9 respectively. The number of time frames is the same as the original movie. The time snapshots for initial, intermediate and final times are shown in figure 9 along with the rose of intersections for the final time for each window size. Window size of 9 gives the best reconstruction among these window sizes at the final time step.

However, we note that a window size of 5 gives good reconstruction for the first time step. While at an intermediate time step, the window size of 5 leads to disruption of grain boundary connectivity and poor reconstruction. On the other hand, window size of 7 gives a reasonable reconstruction for the intermediate time step while it gives an excess of small grains at

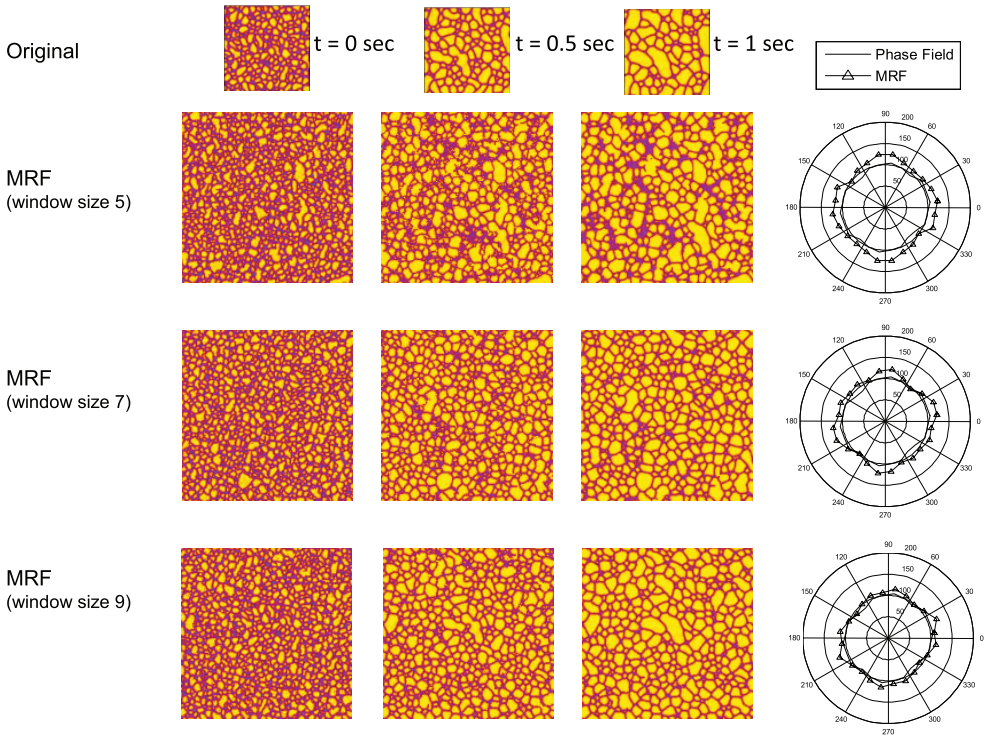

Figure 9. Snapshots of the movie are compared to the synthesized movie snapshots at initial, intermediate and final times. The rose of intersection of the final image at all three steps are also plotted and compared against those of the experimental image.

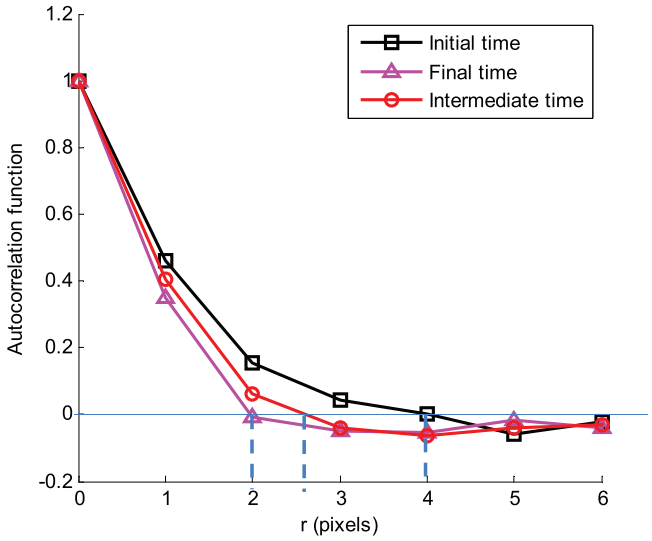

Figure 10. Comparison of autocorrelation function of the phase field simulation at initial, intermediate and final time. The distance at which zero crossover occurs is indicated for the three cases.

the final time step. As shown using the rose of intersections for 3 different window sizes, the technique has no issues with changing grain topology if a sufficiently large window size is chosen in the first step. Since the window size is related to the average grain size, a user could look at the input movie and start with a large enough window. However, one could also start with a smaller window and adaptively increase window sizes during subsequent time steps. An automated way of doing this is to look at the change in correlation functions (treating the polycrystal as two-phase material: grain (phase 1) and grain boundary (phase 2)) over different frames in the movie to adaptively choose the window size. The autocorrelation function of the microstructure is defined as, $\gamma(r) = \frac{S_2(r) - p^2}{p - p^2}$, where p is the volume fraction of phase 1 (the grain boundary phase) and $S_2(r)$ is the two-point correlation measure obtained by randomly placing line segments of length r within the microstructure and counting the fraction of times the end points fall in phase 1, with $p = S_2(0)$ [7]. The autocorrelation functions for the initial, intermediate and final time steps of the original image are plotted in figure 10. The first zero crossover of the autocorrelation function occurs between two and four pixel lengths. The window size chosen should be at least $2z + 1$, where z is the correlation length estimated from the decay of the autocorrelation function. In this case, we use the first zero crossover as the correlation length, which leads to minimal window sizes of 5, 7 and 9 for the initial, intermediate and final time steps for optimal reconstruction. This is reflected in the reconstructions shown in figure 9.

4. Conclusions

We present an extension of our Markov random field algorithm presented in [8] for modelling the temporal evolution of 2D microstructures. We use a movie of microstructure evolution measured over a small window in an experimental sample to estimate the evolution of microstructures over a larger region. The algorithm combines a sampling approach in [8] with a new optimization methodology that allows us to control the microstructural evolution trajectory according to the statistics of the original microstructure movie. In this optimization algorithm, we minimize a neighborhood cost function that ensures that the local neighborhood of the current microstructural frame is similar to some neighborhood in the microstructural movie at any given time step. Three examples were considered for movie synthesis: polycrystalline grain growth from a phase field simulation, a colored movie based on cellular automata simulation of recrystallization, another movie, generated from a phase field simulation, showing non-equiax grains. The snapshots of the microstructures taken at different times from the original movie as well as the synthesized movies were compared. Such a comparison showed that the extended MRF algorithm was able to reproduce the original microstructure simulations while capturing key statistics such as grain size and shape distributions and elastic properties that are representative of the original movie. Such an algorithm, in practise, would decrease the cost of full-scale microstructure measurements by coupling mathematical estimation with targeted small-scale spatiotemporal measurements of microstructure. Future efforts will aim to extend this approach for modeling evolving 3D microstructures.

Acknowledgments

The author would like to acknowledge the Air Force Office of Scientific Research (MURI program) contract FA9550-12-1-0458, for financial support.

References

[1] Heeger D J and Bergen J R 1995 Pyramid-based texture analysis/synthesis *SIGGRAPH 95* pp 229–38
[2] Bonet J S D 1997 Multiresolution sampling procedure for analysis and synthesis of texture images *Proc. SIGGRAPH 97* pp 361–8
[3] Simoncelli E P and Portilla J 1998 Texture characterization via joint statistics of wavelet coefficient magnitudes *Proc. 5th Int. Conf. on Image Processing (Chicago, IL)*
[4] Torquato S 2002 *Random Heterogeneous Materials: Microstructure and Macroscopic Properties* (New York: Springer)
[5] Yeong C L Y and Torquato S 1998 Reconstructing random media II. Three-dimensional media from two-dimensional cuts *Phys. Rev.* E **58** 224–33
[6] Manwart C, Torquato S and Hilfer R 2000 Stochastic reconstruction of sandstones *Phys. Rev.* E **62** 893–99
[7] Sundararaghavan V and Zabaras N 2005 Classification and reconstruction of three-dimensional microstructures using support vector machines *Comput. Mater. Sci.* **32** 223–39
[8] Kumar A, Sundararaghavan V, DeGraef M and Nguyen L 2016 A Markov random field approach for microstructure synthesis *Modelling Simul. Mater. Sci. Eng.* **24** 035015
[9] Bostanabad R, Bui A T, Xie W, Apley D W and Chen W 2016 Stochastic microstructure characterization and reconstruction via supervised learning *Acta Mater.* **103** 89–102
[10] Ising E 1925 Beitrag zur theorie des ferromagnetismus *Z. Phys.* **31** 253–8
[11] Shannon C E 1948 A mathematical theory of communication *Bell Syst. Tech. J.* **27** 379–423
[12] Efros A and Leung T 1999 Texture synthesis by non-parametric sampling *Int. Conf. on Computer Vision* vol **2** pp 1033–8
[13] Popat K and Picard R 1993 Novel cluster-based probability model for texture synthesis, classification, and compression *Visual Communications and Image Processing* pp 756–68
[14] Zhu S, Wu Y and Mumford D 1998 Filters, random fields and maximun entropy (FRAME)—towards a unified theory for texture modeling *Int. J. Comput. Vision* **27** 107–26
[15] Paget R and Longstaff I 1998 Texture synthesis via a noncausal nonparametric multiscale Markov random field *IEEE Trans. Image Process.* **7** 925–31
[16] Mariethoz G and Lefebvre S 2014 Bridges between multiple-point geostatistics and texture synthesis *Comput. Geosci.* **66** 66–80
[17] Sundararaghavan V 2014 Reconstruction of three dimensional anisotropic microstructures from two-dimensional micrographs imaged on orthogonal planes *Integr. Mater. Manuf. Innov.* **3** 1–11
[18] Turner D M and Kalidindi S R 2016 Statistical construction of 3D microstructures from 2D exemplars collected on oblique sections *Acta Mater.* **102** 136–48
[19] Besag J 1974 Spatial interaction and the statistical analysis of lattice systems *J. R. Stat. Soc.* B **36** 192–236
[20] Kwatra V, Essa I, Bobick A and Kwatra N 2005 Texture optimization for example-based synthesis *ACM Trans. Graph.* **24** 795–802 (*Proc. SIGGRAPH*)
[21] Kopf J, Fu C-W, Cohen-Or D, Deussen O, Lischinski D and Wong T-T 2007 Solid texture synthesis from 2D exemplars *SIGGRAPH Proc.* **2** 1–9
[22] Gentry S P and Thornton K 2015 Simulating recrystallization in titanium using the phase field method *IOP Conf. Ser.: Mater. Sci. Eng.* **89** 012024
[23] Liu X and Shapiro V 2015 Random heterogeneous materials via texture synthesis *Comput. Mater. Sci.* **99** 177–89
[24] Vander Voort V F 1993 Examination of some grain size measurement problems *Metallography: Past, Present and Future: 75th Anniversary Volume* (*ASTM Special Technical Publication* vol 1165) (Philadelphia: American Society for Testing and Materials) p 266
[25] Vander Voort V F 1984 *Metallography: Principles and Practice* (New York: McGraw-Hill)
[26] Saltykov S A 1974 *Stereometrische Metallographie* (Leipzig: Deutscher Verlag fur Grundstoffindustrie)
[27] Sundararaghavan V and Zabaras N 2004 A dynamic material library for the representation of single-phase polyhedral microstructures *Acta Mater.* **52** 4111–9
[28] Cellular automaton simulations of grain growth, recrystallization, Max Planck Institut fur Eisenforschung and video is retrieved from www.youtube.com/watch?v=NhfRaLUtvBQ on 17 February 2016

[29] Sundararaghavan V and Zabaras N 2007 Linear analysis of textureproperty relationships using process-based representations of Rodrigues space *Acta Mater.* **55** 1573–87
[30] Sundararaghavan V and Zabaras N 2008 A multi-length scale continuum sensitivity analysis for the control of texture-dependent properties in deformation processing *Int. J. Plast.* **24** 1581–605
[31] Grain Growth/Coarsening During Heating—Using Phase Field Modeling, video is retrieved from www.youtube.com/watch?v=mawloUpGk2o on 8 June 2016